Study of cetyltrialkylammonium bromide and tribromide salts in the solid phase

R. Caminiti,*[a] M. Carbone,[b] G. Mancini[c] and C. Sadun[a]

[a]*Dept. of Chemistry, Istituto Nazionale di Fisica della Materia, University of Rome 'La Sapienza', P.le A. Moro, 5 00185 Rome, Italy*

[b]*Dept. of Chemical Sciences and Technologies, University 'Tor Vergata', Via della Ricerca Scientifica 1, 00133 Rome, Italy*

[c]*Centro CNR di Studio sui Meccanismi di Reazione, C/O Dept. of Chemistry, University of Rome 'La Sapienza', P.le A. Moro, 5 00185 Rome, Italy*

Some cetyltrialkylammonium tribromide salts have been studied in the solid phase using Raman spectroscopy and energy dispersive X-ray diffraction. The first technique detected the presence of asymmetric tribromides while the latter technique revealed the degree of asymmetry of the tribromide units (difference in the bond lengths between external and central Br atoms), by application of a subtraction method. In this method the spectra of the corresponding monobromide salts were recorded and differences between tribromide and monobromide curves isolated the tribromide contributions. The existence of asymmetrical and symmetrical tribromide ions has been established and the degree of asymmetry was then correlated to the steric hindrance and electronegativity of the ammonium substituents. The values of the Br—Br bond distances have been deduced; the most asymmetric tribromide has Br—Br distances at 2.38 and 2.66 Å, while the symmetric tribromide has both Br—Br bond lengths equal to 2.52 Å. A linear geometry is confirmed for the tribromide ions.

The study of polyhalides is important from an applied and a fundamental point of view. Polyhalides are typically used in oxidation reactions of organic molecules as well as for doping polymers in order to change their conductivity.[1]

The number of atoms in a polyhalogen unit can be quite large and depends on the nature of the halogen atom as well as on the hosting structure. Units containing up to seven[2] and eight[3] atoms have been found for polyiodides and up to ten for polybromides.[4]

In all cases a better knowledge of the polybromides structure helps in the understanding of their properties and possible applications. As far as tribromides are concerned, structural studies showed that the tribromide ions usually have linear geometry which can be either symmetric, with the same bond lengths between the external and the central Br atoms [Br(1)—Br(2)=Br(2)—Br(3)], such as in $[(CH_3)_3NH^+]_2Br^-Br_3^-$[5] or asymmetric with different lengths between the external and the central Br atoms [Br(1)—Br(2)≠Br(2)—Br(3)], such as in $CsBr_3$,[6] with a difference of 0.33 Å). The degree of asymmetry is even higher in PBr_7 where the Br_3^- units show bond lengths of 2.39 and 2.91 Å.[7] The degree of asymmetry (the difference between the Br—Br bond lengths) is not constant in different tribromides, but depends on the counter ion and on the host structure.

Several reports, based on Raman spectroscopic evidence, support the existence of tribromide and pentabromide anions.[4,8–10]

Studies on cetyltrimethylammonim tribromide (CTAB3) are reported in ref. 4. The authors indicate the presence, in this molecule, of two Raman bands at 153 and 205 cm^{-1}, which they attribute to Br—Br stretching vibrations, concluding that the Br(1)—Br(2) and Br(2)—Br(3) distances are different. No structural studies on powdered CTA bromide or tribromide have been reported.

We investigate here the degree of asymmetry of the tribromide ion in CTAB3 (sample G1) and in three other quaternary ammonium salts; cetylquinuclidinium tribromide (CQB3, sample G3), cetyltripropylammonium tribromide (CTPAB3, sample G5) and cetyldimethyl(2-hydroxyethyl)ammonium tribromide (CDEAB3, sample G7).

* Email: r.caminiti@caspur.it

Cetyltrymethylammonium bromide (CTAB) is one of the most studied cationic surfactants, used in many fields such as micellar catalysis, medicine and detergency. This surfactant forms micellar aggregates in aqueous solution which are responsible for its useful physico-chemical properties. The corresponding tribromide salt as well as the others we investigated are surfactants used in bromination reactions.[11–15]

The studied quaternary ammonium salts all contain the cetyl ($C_{16}H_{33}$) fragment but differ in the head group so that we investigated the effect of head group variation on the polyhalogen asymmetry.

Study of the polyhalogen asymmetry is usually carried out by a combination of Raman spectroscopy and X-ray diffraction. The stretching vibration frequencies are correlated to the number of atoms in the polyhalogen unit as well as to their structure. For a tribromide the Raman spectra can be used to deduce whether the ion is symmetric or asymmetric.

The X-ray diffraction technique can give information about the structure, thus, in the present case, an exact evaluation of the degree of asymmetry can be achieved.

In the present study we employed both techniques. In particular the degree of asymmetry of the tribromide was determined by large angle X-ray scattering (LAXS). LAXS is a powerful technique for determining structural parameters of non-crystalline systems, since it can provide information about the short-range order.[11–26,30] In particular energy dispersive X-ray diffraction (EDXD)[18–20,22,25,26,29–31] has been found to be a suitable tool in the investigation of such systems due to its high speed and reliability compared to traditional angular scanning X-ray diffraction (ADXD).

For this purpose, X-ray diffraction patterns of the corresponding monobromide samples were collected, and differences evaluated between the curves relative to the tribromide salts and the corresponding monobromide ones. In this way the contribution of the tribromide unit was isolated and analysed.

Experimental

Materials

The CTAB (sample G2), which is commercially available (Fluka) was purified by crystallization from absolute alcohol

and diethyl ether. The cetylquinuclidinium bromide (sample G4) was prepared as reported in ref. 27. The cetyltripropylammonium bromide and the cetyldimethyl(2-hydroxylethyl)ammonium bromide (samples G6 and G8) were prepared by standard quaternization procedures.

The corresponding yellow–orange tribromides were prepared through reaction of the monobromides with Br_2, as reported in ref. 31.

Elemental analyses for H, C, N and Br were performed by the Microanalytical Service of the Area della Ricerca di Roma of the CNR, giving results in agreement with the formulae of the materials (Table 1).

Techniques

Raman spectra. FT Raman spectra (resolution $\pm 4\ cm^{-1}$) of the tribromide salts were recorded on a FRA 106 FT-Raman accessory, mounted on a Bruker IFS 66 FT-IR vacuum instrument, operating with an exciting frequency of 1064 nm (Nd : YAG laser) and with a germanium diode detector cooled at liquid N_2 temperature. Power levels of the laser source varied between 20 and 100 mW. The solid samples were packed into a suitable cell and then fitted into the compartment designed to use 180° scattering geometry. No sample decomposition was observed during the experiments.

X-Ray diffraction patterns. The dispersive X-ray diffraction experiments were carried out by employing a non-commercial X-ray energy scanning diffractometer,[25,26,30] with a solid-state detector, constructed at the Department of Chemistry, University of Rome 'La Sapienza', Powder Diffraction Laboratory.[29] In the design of the machine the goniometer is substituted by two rotating arms, which can be moved independently by a motor in the range of 2θ −5° to 120°, by a program from our group written in BASIC. The X-ray optical path is defined by four Huber 20 μm variable slits mounted on the arms. The distance between the X-ray source and the sample, equal to that between the sample and the detector is 20 cm.

The geometry of our machine is such that both reflection and transmission intensities can be measured.

Advantages of the energy dispersive method over the conventional angle dispersive method have been described[18–20,22,29–31] and the applicability of the method has already been widely described in the literature.[18–20,29,31–33]

A more detailed description of the apparatus has been given in ref. 29 and 30. The X-ray source is a Seifert tube (3 kW) with a tungsten target, which provides X-radiation in the energy range 0–60 keV. The W L lines in the energy range 8–11 keV and the fluorescent X-rays from Br (11.91, 13.29 keV) fall outside of the used energy range. The stability of the voltage power supply for X-rays is better than 0.1%.

The X-ray tube operates at 50 kV and 40 mA for recording the spectra of all samples while conditions of 45 keV and 35 mA were also used for sample G5.

X-Ray detection was accomplished using an EG&G liquid-nitrogen cooled ultrapure Ge SSD (ORTEC, model 92X), connected to a PC 286 *via* ADCAM hardware and Maestro II software, which performs the necessary analogue-to-digital conversions and amplifications. In order to obtain the relation between the photon energy *vs.* the channel number in the multichannel analyser (MCA), the absorption edge of Ba, In, Pd and Eu were used. The linear relationship between the photon energy and the channel number was good.

Measurements

The transmission geometry has been employed, since it allows an easier correction for the sample absorption.[29,30] For measurement of the incident beam spectrum, which is necessary in the energy dispersive method, we used the tube at 50 or 45 kV and 2 mA, while the dimension of the slits was 100 μm × 160 μm.

Fig. 1 shows the primary beam spectrum as well as transmission spectra of samples G7 and G8 measured under the same conditions. Each of the three measurements was recorded over 15 000 s. In order to exclude the fluorescence lines from the spectrum as well as regions where the intensity is strongly absorbed by the sample, the range used in the data analysis was restricted between channel 330 and 680, which corresponds to an energy range of 22.123–45.735 keV. In order to cover a sufficiently wide region of *s*-space ($s = 1.014E\sin\theta$) the diffracted X-ray photons from samples were collected at different scattering angles. Measurement angles and used energy ranges are listed in Table 2.

The scattering intensity was obtained over the range s = 0.2–16.2 $Å^{-1}$. The sample (a pellet of thickness 2 mm) was

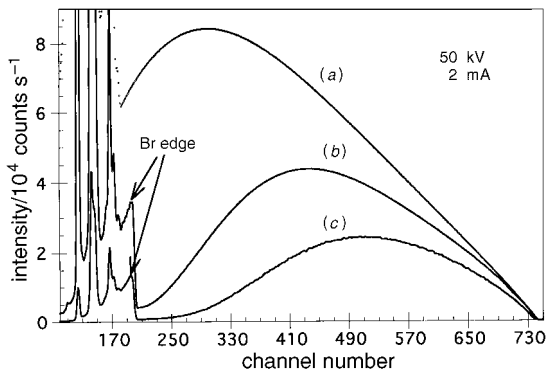

Fig. 1 Energy spectra of the primary beam (*a*), the transmittance of the G8 (*b*) and the G7 (*c*) samples *vs.* channel number in the MCA

Table 1 Elemental analysis[a]

sample	C(%)	N(%)	H(%)	Br(%)
G1 (CTAB3)	42.70	2.8	8.23	42.97
	(43.53)	(2.67)	(8.07)	(45.72)
G2 (CTAB)	61.57	3.99	12.02	24.07
	(62.62)	(3.84)	(11.62)	(21.92)
G3 (CQB3)	47.81	2.50	7.55	42.14
	(47.93)	(2.43)	(8.04)	(41.59)
G4 (CQB)	65.61	3.21	10.07	21.11
	(66.32)	(3.36)	(11.13)	(19.18)
G5 (CTPAB3)	50.31	2.12	8.55	38.69
	(49.35)	(2.3)	(8.95)	(39.40)
G6 (CTPAB)	66.01	3.21	11.97	18.81
	(66.93)	(3.12)	(12.13)	(17.81)
G7 (CDEAB3)	43.01	2.48	7.88	43.45
	(43.34)	(2.53)	(8.00)	(43.25)
G8 (CDEAB)	61.02	3.49	11.09	20.39
	(60.9)	(3.55)	(11.24)	(20.26)

[a]Calculated values in parentheses.

Table 2 Scattering parameters associated with the minimum (22.123 eV) and maximum values (45.735 eV) of the energy for each measurement angle

θ/degrees	s_{min}	s_{max}
21	8.04	16.62
15.5	5.99	12.39
10.5	4.08	8.45
8.0	3.12	6.45
5.0	1.96	4.04
3.5	1.37	2.83
3.0	1.17	2.43
2.0	0.78	1.62
1.5	0.59	1.21
1.0	0.39	0.80
0.5	0.19	0.41

placed at the centre of the goniometer. The measuring time at each angle was set so as to obtain a minimum of 50 000 counts per channel.

Fig. 2 shows, as an example, the diffracted intensity *vs.* the channel number at $\theta=21$, for sample G7. The intensity is plotted in logarithmic scale in order to show also the Br fluorescence lines. Restricting the channel ranges means that the Br fluorescence lines can be excluded from the data analysis range.

Fig. 3 shows diffracted intensities for sample G7 at different collection angles. The transmittance of the sample at $\theta=0°$ has been made under the same experimental conditions as that for the primary beam. The two measurements are necessary to determine the sample linear absorption coefficient, which varies to a significant extent with the X-ray energy. From the relation

$$I_t(E)/I_0(E)=\exp[-\mu(E)t]$$

we obtain the experimental values of $\exp[-\mu(E)t]$ used in eqn. (1) and (2) for absorption corrections.[30,31]

The total intensity I' scattered by a sample and observed by the energy dispersive detector in approximation of single scattering and transmission geometry[25,30,31] can be expressed as:

$$I'(E,\theta)=KI_0(E)P(E,\theta)A_{Coh}(E,\theta)I(E,\theta) \quad (1)$$

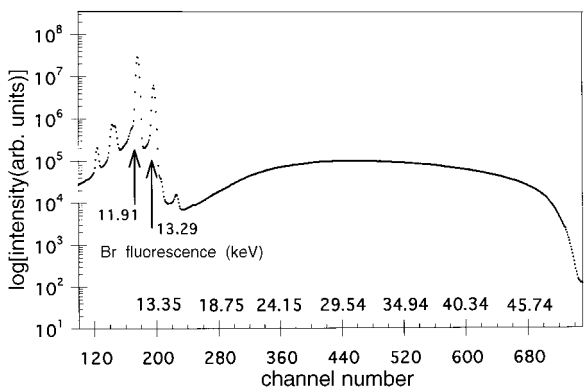

Fig. 2 EDXD profile of the sample G7 obtained at $\theta=21$

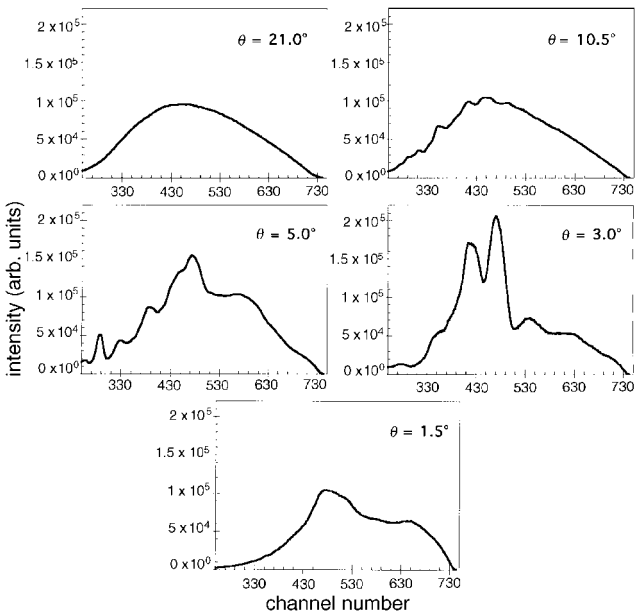

Fig. 3 EDXD profiles of the sample G7 obtained at different collection angles

with

$$I(E,\theta)=I_{Coh}(E,\theta)+\frac{E'I_0(E')P(E',\theta)A_{Inc}(E,E',\theta)I_{Inc}(E',\theta)}{EI_0(E)P(E,\theta)A_{Coh}(E,\theta)} \quad (2)$$

where θ is the scattering angle, E is the photon energy revealed by the detector and E' is the initial energy of a photon inelastically scattered at the observed energy E; K is the scale factor between the intensity reaching the detector and the intensity scattered by a stoichiometric unit of sample; $I_0(E)$ is the energy spectrum of the primary beam measured at $\theta=0°$; $P(E,\theta)$ is the polarization factor by a scattering of primary radiation with polarization $\Pi(E)$, $I_{Coh}(E,\theta)$ is the total scattered elastic intensity and to which three different terms contribute [eqn. (3)], where $\Sigma_i c_i f_i^2(s)$ is the self-scattering intensity; c_i is the concentration of the different species, $i_1(s)$ and $i_2(s)$ are the intensities of interfering waves scattered by atom pairs belonging to the same and different domains respectively; s is the scattering parameter and is defined by eqn. (4),

$$I_{Coh}(E,\theta)=\sum_n c_i f_i^2(s)+i_1(s)+i_2(s) \quad (3)$$

$$s=4\pi\sin\theta/\lambda=1.014\ E\sin\theta \quad (4)$$

where E is expressed in keV and s in $Å^{-1}$. A more detailed description of the terms reported in eqn. (1) and (2) has been given in ref. 25 and 29–31.

Data treatment

After correction of the collected experimental data, for escape peak suppression, the intensity data were handled, as described by Nishikawa and Iijima,[31] by means of our DIF1 program written in Fortran IV. Normalization to a stoichiometric unit of volume containing one Br atom was performed. Radial distribution functions $D(r)$, were calculated from the static structure functions $i(s)$ [eqn. (5)], according to eqn. (6).

$$i(s)=I_{coh}(E,\theta)-\sum_i c_i f_i^2(s) \quad (5)$$

$$D(r)=4\pi r^2\rho_0+2r\pi^{-1}\int_0^{s_{max}} s.i(s).M(s)\sin(rs)\,ds \quad (6)$$

In this equation $\rho_0=[\Sigma_i n_i f_i(0)]^2V^{-1}$, where V is the stoichiometric unit of volume chosen, n_i = number of atoms i per unit volume, and f_i the scattering factor per atom i. The sharpening factor is given by eqn. (7).

$$M(s)=\{f_{Br}^2(0)/f_{Br}^2(s)\}\exp(-0.005\ s^2) \quad (7)$$

In order to determine the Br—Br bond lengths in the tribromomide ions, the peaks referring to the Br—Br interactions were isolated by a subtraction method.[34–36] By subtracting the radial distribution function of the monobromide ammonium salts from the corresponding tribromide salts, we have obtained a difference radial distribution function that contains information selectively about the Br first neighbours in the range 0–3 Å. The resulting difference curves are indicated as $D(r)_{Br_3}-D(r)_{Br}$.

The subtraction operation is valid only if the organic structure is unaltered by the presence of two extra bromine atoms, so that its contribution to the radial distribution function remains the same both in the mono- and in the tribromide salts. The absence, in the difference curve, of extra oscillations with respect to the original curves or of negative peaks indicates the correctness of this hypothesis.

Theoretical peaks were calculated, by a corresponding Fourier transformation of the theoretical intensities for pairs of interactions between atoms p and q (Debye functions) [eqn. (8)], using the same sharpening factor and the same s_{max}

value as for the experimental data and assuming the root mean square deviation to be σ_{pq}.

$$i_{pq}(s) = \sum f_p f_q \sin(r_{pq}s)\,(r_{pq}s)^{-1} \exp(-0.5\,\sigma^2{}_{pq}s^2) \qquad (8)$$

Since our goal was the determination of Br—Br distances within the tribromide ion we considered the Debye functions only for Br—Br first neighbour interactions.

Data analysis

Raman spectra

The Raman spectra of the studied samples are shown in Fig. 4 and observed vibration frequencies of the Raman-active bands are collected in Table 3, where also a comparison to literature data for symmetric tribromides is made. Large shifts in both the wavenumber and intensity of the bands are observed and appear to correlate with the degree of asymmetry in the two Br—Br bond lengths.

The vibrational spectra of tribromides can be viewed in terms of interaction of Br_2 with Br^- with the latter acting as a Lewis base and Br_2 as a Lewis acid. Upon complexation of Br_2 with Br^-, Br—Br antibonding molecular orbitals are populated and the Br—Br bonds weakened; hence the Br—Br distance is increased from 2.3 Å in Br_2 [37] to 2.53 Å, for instance, in $(C_6H_5)_4As^+Br_3^-$,[39] and the resulting constant force is lowered significantly from that in Br_2.

The Raman spectrum of Br_2 in benzene,[8] yields a fundamental stretching frequency at 306 cm^{-1}, while, for symmetrical Br_3^- units (with equal Br—Br distances) such as in $(n\text{-}C_4H_9)N^+Br_3^-$, the actual Br—Br stretching frequency is 179 cm^{-1}, and is the average of symmetrically and antisymmetrically coupled normal modes.[39]

The vibration frequencies differ for asymmetrical Br_3^- units and the two stretching modes are observed separately. In $CsBr_3$,[6] which shows two different Br—Br bond distances of 2.44 and 2.77 Å, the vibration frequencies were observed at 140 and 208 cm^{-1}. In a more asymmetrical tribromide such as $PBr_4^+Br_3^-$,[7] where the Br—Br bond lengths are in the range 2.39–2.91 Å, the stretching frequencies are observed[40] at 249–135 cm^{-1}.

Apparently, the splitting between the vibration frequencies can be correlated to the degree of asymmetry and can be considered a qualitative method to deduce whether the tribromide ion is symmetrical or asymmetrical.

Within this simple picture, samples G1 and G7, with stretching vibration frequencies of 153, 205 and 140, 223 cm^{-1}, respectively, contain asymmetrical Br_3^- units, with most probably, a higher degree of asymmetry in sample G7 (larger splitting between the vibration frequencies).

Sample G3 might contain a symmetrical Br_3^- unit since a coupled vibration frequency is observed at 163 cm^{-1}. This value is somewhat different from the value of 179 cm^{-1} reported for $(n\text{-}C_4H_9)N^+Br_3^-$,[39] but this may simply depend on the Br—Br bond distance, which we have calculated for the sample G3, but is not reported for $(n\text{-}C_4H_9)N^+Br_3^-$. Sample G5 shows somewhat unusual behaviour in that the two vibration frequencies of 168 and 226 cm^{-1} do not follow the usual trend, of a lower stretching frequency for the ν_1 vibration and higher frequency for ν_3 compared to the average frequency for symmetric units. Furthermore at increasing asymmetry the intensity of the peak corresponding to the ν_3 vibration increases as does as the intensity ratio ν_3/ν_1 (see ref. 4 Fig. 1). For sample G7, instead, the ν_1 vibration is more intense. To be sure that both the peaks refer to the sample and not, for instance, to a symmetric Br_3^- (with a stretching vibration at 168 cm^{-1}), with an impurity yielding a peak at higher vibration frequency a newly prepared sample was analysed, which yielded a similar Raman spectrum and diffraction pattern. In this case we consider the Raman spectrum is not sufficient to discriminate whether the tribromide unit is asymmetrical. The splitting of the frequencies for sample G7 hints rather at resonance effects, which can occur when two vibrations have closely spaced frequencies

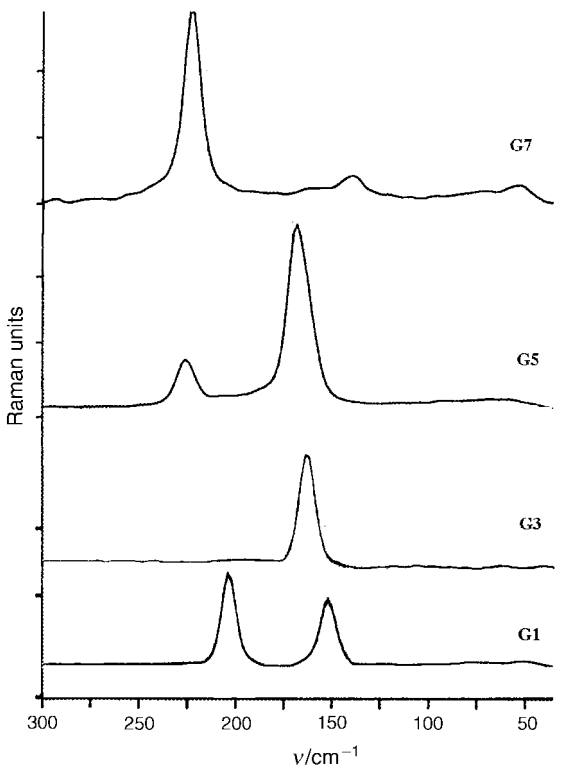

Fig. 4 Raman spectra of the tribromide salts. Sample G3 shows one peak only and hints at symmetric tribromide. The samples G1, G5 and G7 show two peaks, which suggest the presence of asymmetric tribromides, though the splitting and the intensity ratios are not the same

Table 3 Stretching frequencies of the tribromide Raman-active vibrations

sample	cation	ν_1/cm^{-1}	ν_3/cm^{-1}	ref.
G1	CTA	153	205	
	CTA	153	205	4
G3	CQ	163		
G5	CTPA	168	226	
G7	CDEA	140	223	
	Cs^+	138	213	8

X-Ray diffraction patterns

Observed structure functions, in the form $s.i(s).M(s)$ are shown in Fig. 5 for samples G1 and G2. Below 3 $Å^{-1}$ the curves for the monobromide and tribromide salts show similar structures,

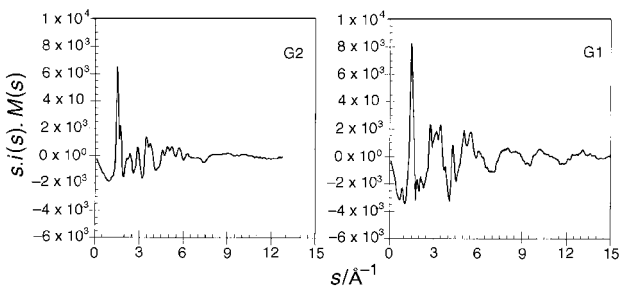

Fig. 5 Observed structure function $s.i(s).M(s)$ of samples G2 and G1. The structure function of the tribromide sample shows much wider oscillations compared to the corresponding monobromide one.

whereas much wider oscillations are seen for the tribomide in the range 3–15 $Å^{-1}$, hinting at the presence of extra interactions not present in the monobromides, most probably due to the first neighbour Br—Br interactions. No significant difference in the reduced intensities is displayed by different samples.

The radial distribution functions in the Diff form [Diff(r)= $D(r)-4\pi r^2\rho_0$] are shown in Fig. 6 for the monobromides in and Fig. 7 for the tribromides in the range 0–15 Å. However we only analysed the region 0–3 Å where we can distinguish the first-neighbour Br—Br interactions. The distribution functions of the monobromide samples show two peaks at *ca.* 1.5 and 2.5 Å arising from C···C, and N—C bond distances (*ca.* 1.5 Å), and the non-directly bound C···C and N—C distances, with sp^3 hybridization (*ca.* 2.5 Å) calculated for the organic substituents of the ammonium cation.

In the radial distribution functions of the tribromides, the area of the peak at *ca.* 2.5 Å is much larger, compared to the corresponding monobromide curves, therefore cannot be simply ascribed to the C···C interaction, but it must contain the contribution of a higher scattering species, namely a Br—Br interaction. The literature data related to Br—Br distances in tribomide ions, both for symmetric and asymmetric units are in agreement with such a value, therefore we consider that the comparison of this peak to theoretical peak shapes yields the Br—Br bond distances.

Another typical feature in the tribromides RDF is a peak at *ca.* 5.1 Å, which we ascribe to Br(1)···Br(3) interactions, since it is rather intense and has no correspondence in the monobromide curves. The position of this peak confirms that the anion Br_3^- has a linear geometry, as suggested in a previous EXAFS study.[1]

Fig. 8(*a*) shows the radial distribution function of samples G1 and G2 in the range 0–5.5 Å, compared to the theoretical peak shapes calculated for the monobromide. In this calculation we have considered interactions of the type C—X, with X=C, N, O between all the first and second neighbours. Particularly for the C···C interaction we considered the CTAB structure determined by Campanelli and Scaramuzza[41] in which the C—X distances used in the calculations are reported. The experimental curve is well reproduced by the calculated peak shapes in the 0–2.7 Å range, indicating that the considered interactions are sufficient to simulate the RDF of the monobromide ammonium salts. Therefore the subtraction of the monobromide RDF from the corresponding tribromide RDF simply yields the peaks related to Br—Br interactions. If any change in the cation geometry occurs when coordinated to a tribromide, instead of a monobromide ion or if some interactions are present in the monobromide ion, which disappear for the tribromide, this would result, either in a residual peak and/or in a negative peak.

The peak at *ca.* 1.5 Å can be used to determine if the subtraction operation is valid. As shown in Fig. 8(*b*) for sample G1 the difference radial distribution function is fairly flat in the range 0–2 Å and the difference radial distribution functions for the other samples show the same characteristics. We can, therefore, consider that the subtraction of the monobromide

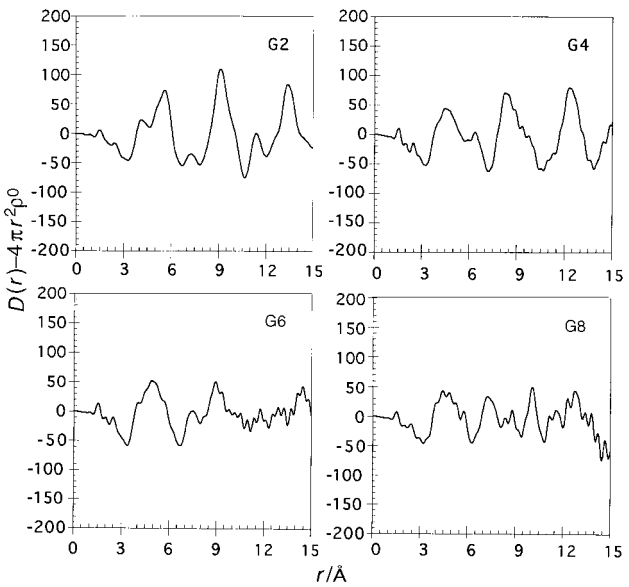

Fig. 6 Radial distribution functions of the form $D(r)-4\pi r^2\rho_0$ of the monobromide samples

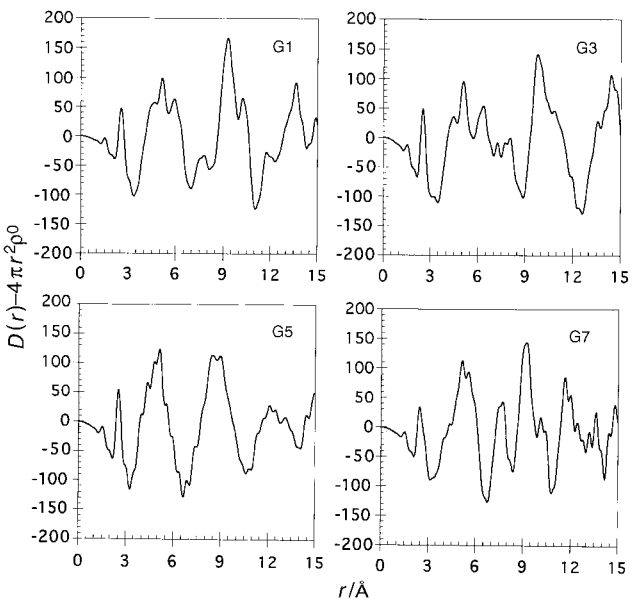

Fig. 7 Radial distribution functions of the form $D(r)-4\pi r^2\rho_0$ of the tribromides samples

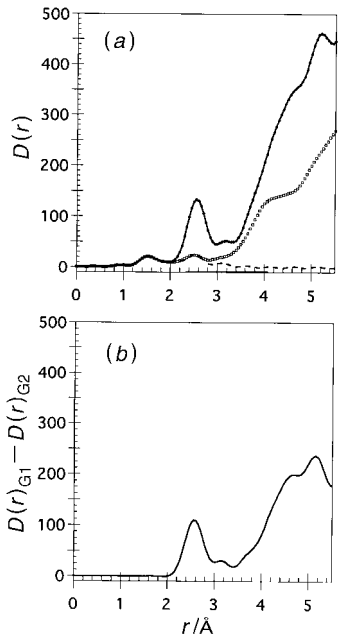

Fig. 8 (*a*) Dotted line, $D(r)$ of the sample G2 in the range 0–5.5 Å; continuous line, $D(r)$ of the sample G1; dashed line, theoretical peak shape calculated by introducing in the Debye formula the first- and second-neighbour interactions of the ammonium cation, which is common to both samples. (*b*) Difference curve between the radial distribution functions of sample G1 and G2 [$D(r)_{G1}-D(r)_{G2}$]. The difference curve in the range 0–2 Å is rather flat, therefore all contributions of the ammonium cation have been removed by subtraction.

curve isolates only the Br—Br contribution to the tribromide RDF and that the calculation of theoretical peak shapes, which reproduces the peak at *ca.* 2.5 Å in the difference curve should give exact Br—Br distances. This operation was performed for all the samples and the corresponding Br—Br distances are reported in Table 4, together with mean square root used in the calculation. In Fig. 9 the experimental and theoretical difference curves have been reported for all the sample pairs, and show good agreement. The presence of a peak at *ca.* 5.1 Å in the tribromide RDF allows us to infer the Br_3^- geometry.[1] This peak, which we consider correlated to a Br···Br interaction, corresponds to the sum of the Br—Br distances in both symmetric and asymmetric units. The only possible geometry that would yield peaks at a distance twice the fundamental one, is linear.[1] The theoretical $s.i(s).M(s)$ curves have been calculated by introducing only interactions related to the Br_3^- unit, in the Debye formula [eqn. (8)], using the parameters reported in Table 4. From this we can see how, despite the similarities between the samples (they are all ammonium salts with a long aliphatic chain) symmetric (G3), slightly asymmetric (G5), and highly asymmetric (G1, G7) structures are all observed.

Finally, theoretical curves are compared to experimental ones in Fig. 10 for samples G1 and G3.

It is of interest how the use of these interactions is already sufficient to reproduce the oscillations of the structure functions in the entire range, that is, by contrast quite flat for the corresponding monobromides, clearly indicating that the Br_3^- ion gives the main contribution to the scattered intensity.

Results and Discussion

In the previous sections we showed that the studied samples display different degrees of asymmetry of the tribromide ion.

Table 4 Br—Br bond lengths in Br_3^- and the corresponding root mean square deviation. σ_1, σ_2 and σ_3 refer to the Br(1)—Br(2), Br(2)—Br(3) and Br(1)—Br(3) bond lengths respectively

sample	Br(1)—Br(2) /Å	Br(2)—Br(3) /Å	Br(1)—Br(3) /Å	$\sigma_1=\sigma_2$	σ_3
G1	2.45	2.66	5.11	0.08	0.15
G3	2.52	2.52	5.04	0.11	0.15
G5	2.48	2.55	5.03	0.10	0.14
G7	2.38	2.66	5.04	0.08	0.15

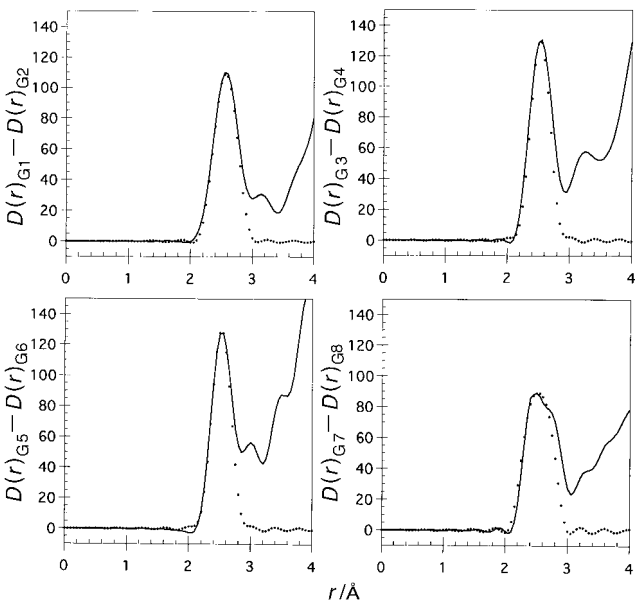

Fig. 9 Difference radial distribution curves: solid lines, experimental curves; dotted lines, theoretical curves

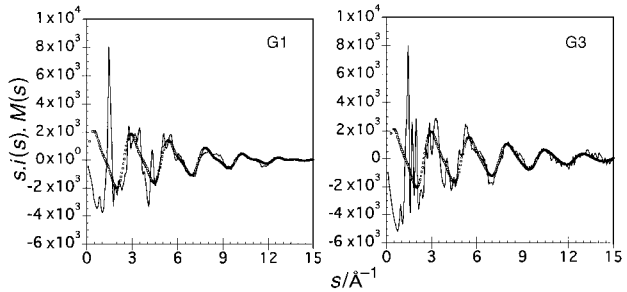

Fig. 10 Comparison between observed (solid lines) and calculated (dotted lines) structure functions $s.i(s).M(s)$ for G1 and G3

For instance the difference between the Br(1)—Br(2) and Br(2)—Br(3) distances is 0.00 Å in sample G3 and 0.28 Å in sample G7. Furthermore the latter value is comparable to the situation where Cs^+ is the counter ion.

The degree of asymmetry in the tribromide ions is correlated to their geometry with respect to the cation as well as to its electronegativity. The asymmetry can be viewed as a preferential interaction of one of the external Br atoms with the cation, which can induce a polarization of the Br—Br bonds. The effect of the electronegativity is quite evident for instance in $CsBr_3$,[6] where an electropositive atom such as Cs^+, causes a high degree of asymmetry.

In quaternary ammonium salts with hydrocarbon chains, electronegativity is not particularly important for the Br—Br bond polarization and the asymmetry is simply connected to the orientation of the linear Br_3^- unit relative to the nitrogen atom. A completely symmetrical surrounding of the nitrogen atom leads to a symmetric tribromide such as in $(n\text{-}C_4H_9)N^+Br_3^-$.[39]

The investigated samples all contain a long aliphatic chain (the cetyl fragment), which introduces an element of asymmetry around the nitrogen atom, since the other substituents around the nitrogen are small. In the cetyltrimethylammonium salt this degree of asymmetry is high and, correspondingly, the tribromide asymmetry is high. In the cetyltri-*n*-propyl ammonium salt the length of the substituents is already sufficient to prevent a preferential interaction of one Br end with the nitrogen and this tribromide is almost symmetric.

The behaviour of the cetylquinuclidinium ammonium salt is interesting, in that despite its apparent geometrical asymmetry a symmetric tribromide is observed. Most probably the aliphatic chains are forced into a ring geometry, leaving space for the nitrogen atom to adopt a similar interaction with both external Br atoms.

The high degree of asymmetry for the cetyldimethyl(2-hydroxyethyl)ammonium is not surprising, since the geometrical asymmetry around the nitrogen atom is accompanied by the presence of an electronegative element, oxygen, which can polarize the Br—Br bonds.

It is interesting to note the good correspondence between the Raman spectra and the X-ray diffraction patterns, with a single stretching vibration frequency for symmetric tribromides and split vibration frequencies for highly asymmetric tribromide units. The slight asymmetry in sample G5 might have induced, as previously suggested, a Fermi resonance.

In summary we studied the dependence of the degree of asymmetry of tribromides on the substituents of ammonium salts, by Raman spectroscopy and large angle scattering. The results show that the electronegativity of the ammonium substituent can polarize one Br external atom, yielding Br—Br bonds of different length.

However even with non-polar substituents it is possible to obtain asymmetric tribromides, depending on the steric hindrance and on the possibility for the tribromide units to

interact with the nitrogen atom either asymmetrically or symmetrically. In all cases the tribromide geometry was linear.

Dr. Luca Antonio Petrilli and Mr. Franco Dianetti of the Servizio Microanalisi, Area della Ricerca di Roma of the CNR are acknowledged for their kind contribution.

References

1 H. Oyanagy, M. Tokumoto, T. Ishiguro, H. Shirakawa, H. Nemoto, T. Matsuita, M. Ito and H. Kuroda, *J. Phys. Soc. Jpn*., 1984, **53**, 4044.
2 F. Demartin, P. Deplano, F. A. Devillanova, F. Isaia, V. Lippolis and G. Verani, *Inorg. Chem*., 1993, **32**, 3694.
3 E. E. Having, K. H. Boswijk and E. H. Wiebenga, *Acta Crystallogr*., 1954, **7**, 487.
4 G. R. Burns and R. M. Renner, *Spectrochim. Acta, Part A*, 1991, **47**, 991.
5 C. Romers and E. W. M. Keulemans, *Proc. K Ned. Akad. Wet., Ser B*, 1958, **61**, 345.
6 G. L. Breneman and R. D. Willet, *Acta Crystallogr., Sect. B*, 1969, **25**, 1073.
7 G. L. Breneman and R. D. Willet, *Acta Crystallogr., Sect. B*, 1967, **23**, 467.
8 D. W. Kalina, J. W. Lyding, M. T. Ratajack, C. R. Kannewurf and T. J. Marks, *J. Am. Chem. Soc*., 1980, **102**, 7854.
9 J. C. Evans and G. Y. S. Yo, *Inorg. Chem*., 1967, **6**, 1483.
10 A. Schnittke, H. Stegemann, H. Fuellbier and J. Gabrusenoks, *J. Raman Spectrosc*., 1991, **22**, 627.
11 G. Cerichelli, C. Grande, L. Luchetti, G. Mancini and C. A. Bunton, *J. Org. Chem*., 1987, **52**, 5167.
12 M. T. Bianchi, G. Cerichelli, G. Mancini and F. Marinelli, *Tetrahedron Lett*., 1984, **25**, 5205.
13 G. Cerichelli, L. Luchetti and G. Mancini, *Tetrahedron Lett*., 1989, **30**, 6209.
14 G. Cerichelli, C. Grande, L. Luchetti and G. Mancini, *Org. Chem*., 1991, **56**, 3025.
15 G. Cerichelli, L. Luchetti and G. Mancini, *Tetrahedron*, 1996, **52**, 2465.
16 J. J. Del Val, L. Esquivias, P. L. Olano and F. Sanz, *J. Non-Crystalline Solids*, 1985, **70**, 211.
17 A. Corrias, G. Ennas, G. Licheri, G. Marongiu, A. Musinu, G. Paschina, G. Piccaluga and G. Pinna, *J. Mater. Sci. Lett*., 1988, **7**, 407.
18 T. Egami, *J. Mater. Sci*., 1978, **13**, 2587.
19 T. Egami, in *Glassy metals I*, ed. H. J. Gunterodt and H. Beck, Springer Verlag, Berlin, 1981, p. 25.
20 G. Fritsch and J. Keimel, *Mater. Sci. Eng., A*, 1991, **134**, 888.
21 F. Haydu, *Phys. Status Solidi A*, 1980, **60**, 365.
22 T. Egami, *J. Appl. Phys*., 1979, **50**, 1564.
23 A. Mosset, J. Galy, E. Coronado, M. Drillon and D. Beltran, *J. Am Chem. Soc*., 1984, **106**, 2864.
24 R. Caminiti, C. Munoz Roca, D. Beltran-Porter and A. Rossi, *Z. Naturforsch., Teil A*, 1988, **43**, 591.
25 A. Capobianchi, A. M. Paoletti, G. Pennesi, G. Rossi, R. Caminiti and C. Ercolani, *Inorg. Chem*., 1994, **33**, 4635.
26 D. Atzei, D. De Filippo, A. Rossi, R. Caminiti and C. Sadun, *Spectrochim. Acta, Part A*, 1995, **51**, 11.
27 R. Germani, P. P. Ponti, T. Romeo, G. Savelli, N. Spreti, G. Cerichelli, L. Luchetti, G. Mancini and C. A. Bunton, *J. Phys. Org. Chem*., 1989, **2**, 553.
28 G. Cerichelli, G. Mancini and L. Luchetti, *Tetrahedron*, 1994, **50**, 3797.
29 (*a*) R. Caminiti, C. Sadun, V. Rossi, F. Cilloco and R. Felici, *XXV National Congress of Chemical Physics*. Cagliari, 1991; (*b*) Pat. 01261484, June 23, 1993.
30 M. Carbone, R. Caminiti and C. Sadun, *J. Mater. Chem*., 1996, **6**, 1709.
31 K. Nishikawa and T. Iijima, *Bull. Chem. Soc. Jpn*., 1984, **57**, 1750.
32 K. Nishikawa and N. Kitagawa, *Bull. Chem. Soc. Jpn*., 1980, **53**, 2804.
33 V. Petkov and Y. Woseda, *J. Appl. Crystallogr*., 1993, **26**, 295.
34 R. Caminiti, G. Johansson and I. Toth, *Acta Chem. Scand., Ser. A*, 1986, **40**, 435.
35 G. Johansson and R. Caminiti, *Z. Naturforsch., Teil A*, 1986, **41**, 1325.
36 R. Caminiti, F. Cilloco and R. Felici, *Mol. Phys*., 1992, **75**, 681.
37 C. Andreani, F. Cilloco, L. Nencini, D. Rocca and R. N. Sinclair, *Mol. Phys*., 1985, **55**, 887.
38 G. Ollis, V. J. James, D. Ollis and M. P. Boogard, *Cryst. Struct. Commun*., 1976, **5**, 39.
39 W. Gabes and H. Gerding, *J. Mol. Struct*., 1972, **14**, 267.
40 W. Gabes and H. Gerding, *Recl. Trav. Chim. Pays-Bas*, 1971, **90**, 157.
41 A. R. Campanelli and R. Scaramuzza, *Acta Crystallogr., Sect. C*, 1986, **42**, 1380.

Paper 6/04726B; *Received* 5*th July*, 1996